Enantiorecognition of a new chiral selector, β-cyclodextrin perphenylcarbamate, as studied by NMR spectroscopy and molecular energy calculation

Yoshihiro Kuroda,*[a] Yoshiyuki Suzuki,[a] Jingyi He,[a] Takahiro Kawabata,[a] Akimasa Shibukawa,[a] Hiroo Wada,[b] Hiroya Fujima,[b] Yasuhiko Go-oh,[c] Eiji Imai[c] and Terumichi Nakagawa[a]

[a] *Faculty of Pharmaceutical Sciences, Kyoto University, Sakyo-ku, Kyoto 606, Japan*
[b] *Shinwa Chemical Industries Ltd., Kagekatsu-cho 50, Fushimi-ku, Kyoto 612, Japan*
[c] *Taiyo Pharmaceutical Industry Co. Ltd., Aoi 3-24-2, Higashi-ku, Nagoya 461, Japan*

The mechanism of enantioselective binding of chiral atenolol (AT) by β-cyclodextrin perphenylcarbamate (PhCD) has been studied by NMR spectroscopy and by molecular modelling techniques including conformational and free energy of binding calculations for the AT–PhCD complexes. Among the various models tested, the (*R*)-enantiomer was found from the calculations to bind with the PhCD with its asymmetric carbon moiety inside the toroid of cyclodextrin, while its aromatic ring is outside the toroidal cavity at the secondary hydroxy group side; in contrast, the (*S*) counterpart preferred to locate its aromatic ring inside the toroid, while retaining the asymmetric carbon moiety outside the cavity at the primary hydroxy group side. The differential changes in ^{1}H NMR chemical shifts and linewidths between the enantiomers of AT, caused as a result of interaction with PhCD, clearly reflected the difference in the binding mode suggested from the present molecular modelling calculations. It was concluded that although the binding affinity of (*S*)-AT is weaker than that of (*R*)-AT, the mobility of the (*S*)-enantiomer is lowered more than the (*R*) counterpart as a result of the interaction with PhCD.

Almost half of the commercially available drugs have a chiral centre, and a half of them are clinically used as racemates.[1,2] Not only pharmacological but pharmacokinetic and pharmacodynamic activities of a drug are based on the biological interaction between the drug and biopolymers such as plasma and tissue proteins, enzymes and receptors. These biopolymers generate the field of chiral recognition based on the diastereoisomeric interaction with a chiral drug. Since the stability of the diastereoisomeric complex is different between drug isomers, the pharmacokinetic and pharmacodynamic characteristics of a chiral drug are potentially stereoselective. For keeping the effectiveness and safety of chiral drugs, the stereoselective studies on their pharmacokinetics and pharmacodynamics are important, and hence a simple and easy analytical method for the chiral separation is of practical demand.

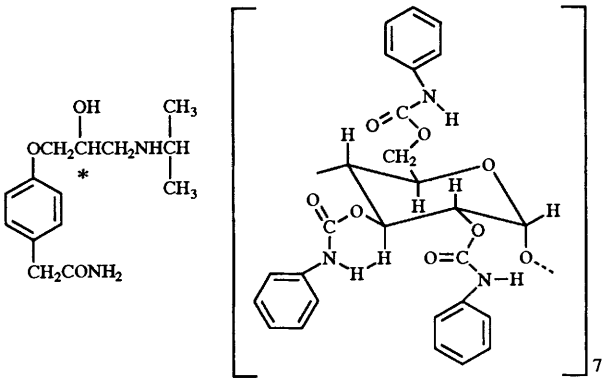

ATENOLOL PhCD

Atenolol is a cardioselective β-adrenoceptor blocking agent (β-blocker). Atenolol has a chiral centre, and is clinically used as a racemate. However, like most other β-blockers, the pharmacological activity resides in the (*S*)-enantiomer. Several HPLC methods have been reported for the enantioselective determination of atenolol in biological fluids; such as reversed-phase HPLC after chiral derivatization[3–7] and HPLC on a chiral stationary phase [α_1-acid glycoprotein immobilized silica[8] or (*R,R*)-diaminocyclohexane–dinitrobenzoyl chiral stationary phase[9]] after an achiral derivatization. It is reported that a β-cyclodextrin immobilized column resolves atenolol enantiomers with a mobile phase consisting of a mixture of polar organic solvents (acetonitrile–methanol–acetic acid–triethylamine), although this column did not allow the enantioseparation under aqueous mobile phase conditions.[10] Recently, we developed a novel on-line HPLC system for the enantioselective determination of atenolol in plasma following direct sample injection.[11] This system consists of a pretreatment column which separates atenolol from endogenous plasma components, and extraction column which traps atenolol in the eluent fraction from the pretreatment column, and a chiral selector column which resolves atenolol enantiomers without derivatization. This HPLC system allows a reliable and reproducible analysis, which was confirmed by the validation tests of within-day and day-to-day analyses. This HPLC system was applied to measure the time courses of atenolol enantiomer concentrations in human plasma after oral administration. The chiral selector used in this system is a newly developed β-cyclodextrin perphenylcarbamate (PhCD)-bonded silica column. The chiral separation is based on the enantioselective interaction between atenolol and PhCD.

In this paper, NMR measurements and a molecular energy calculation technique were applied in order to delineate this chiral recognition mechanism from a view-point of molecular structures of the atenolol–PhCD complex. The total energy and the free energy of binding (dG) values of atenolol and PhCD interaction *via* several complex models were calculated to determine the most stable complex formation.

Experimental

Chemicals and materials

β-Cyclodextrin (β-CD) was purchased from Wako Pure Chemical Industries (Osaka, Japan). Phenyl isocyanate was

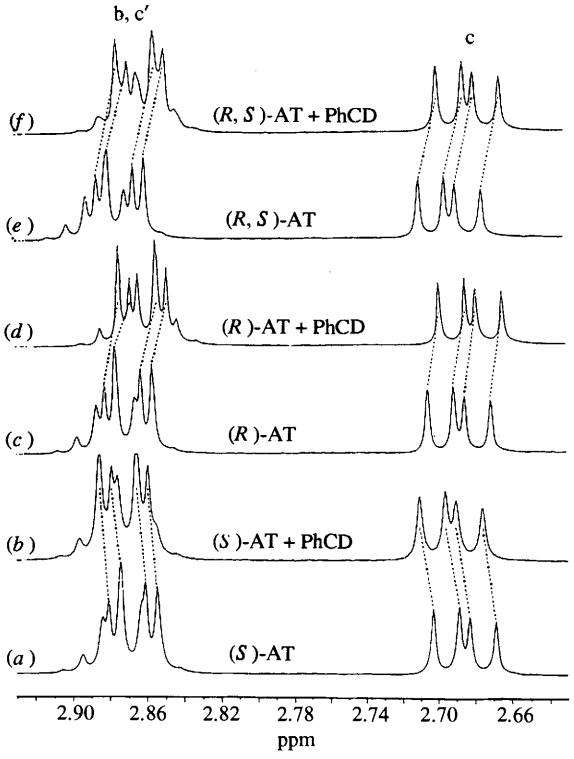

Fig. 1 ^{1}H NMR spectra of b, c and c' protons of atenolol (300 K). (*a*) 5 mmol dm^{-3} (*S*)-atenolol; (*b*) 5 mmol dm^{-3} (*S*)-atenolol and 5 mmol dm^{-3} PhCD; (*c*) 5 mmol dm^{-3} (*R*)-atenolol; (*d*) 5 mmol dm^{-3} (*R*)-atenolol and 5 mmol dm^{-3} PhCD; (*e*) 5 mmol dm^{-3} (*R,S*)-atenolol; (*f*) 5 mmol dm^{-3} (*R,S*)-atenolol and 5 mmol dm^{-3} PhCD.

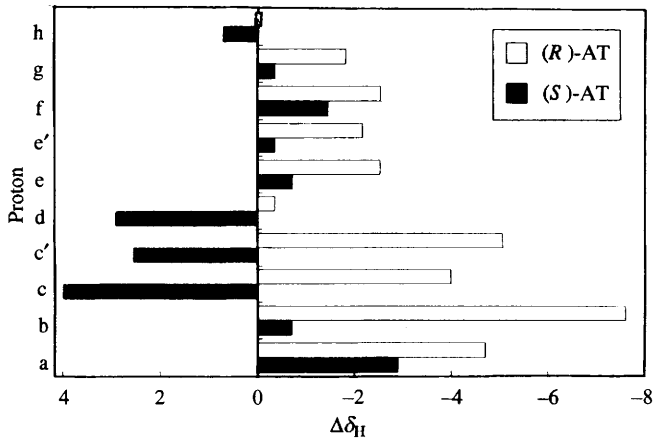

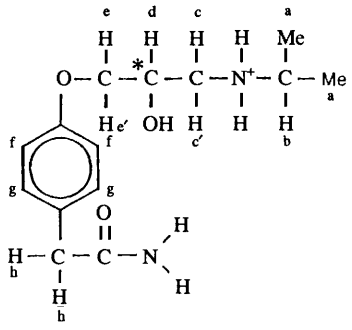

Fig. 2 Changes in chemical shifts ($\Delta\delta$/Hz) of atenolol on interaction with PhCD (300 K)

purchased from Tokyo Kasei Kogyo Co. Ltd. (Tokyo, Japan). Other solvents used in the preparation of PhCD were at least analytical-reagent grade and carefully dried before use.

Preparation of PhCD

β-CD (0.57 g), dried at 80 °C under vacuum for 8 h, was dissolved with stirring in 10 cm^3 of dry pyridine. To this solution, phenyl isocyanate (1.4 g) was added with stirring. After 8 h at 80 °C, the phenylcarbamoylated compound was precipitated in methanol–water (1:1, v/v), filtered, vacuum dried at 80 °C for 8 h, and was recrystallized successively from tetrahydrofuran, pyridine, water and hexane. Elemental analysis data supported the formation of completely carbamoylated β-CD (Found: C, 62.7; H, 5.0; N, 8.4. Calc.: C, 62.4; H, 4.8; N, 8.1%).

NMR measurements

The ^{1}H NMR spectra of atenolol (5 mmol dm^{-3}) and atenolol (5 mM)–PhCD (5 mM) solutions were measured on a Bruker AM-600 (600 MHz) spectrometer. The sample solutions were prepared by dissolving atenolol and/or PhCD in the mixed solvents of [$^2H_4$]methanol and DCl; the apparent pH of the solutions was 2.5 (meter reading). The chemical shifts were referenced to the residual CHD_2 proton (3.31 ppm) of [$^2H_4$]methanol. Measurements were made at both 300 and 283 K. Digital resolution was 0.36 Hz/point.

Results

^{1}H NMR spectra at 300 K

The ^{1}H NMR spectra of both (*S*)- and (*R*)-atenolol solutions showed almost no changes in chemical shifts and linewidths on addition of PhCD to those solutions, suggesting that the interactions between atenolol and PhCD were very weak in the presently employed experimental conditions. However, we noticed slight differences in the chemical shifts of atenolol as a result of interaction with PhCD. Fig. 1 shows a typical example for the ^{1}H NMR spectra for protons c, c' and b of atenolol in the absence (spectra *a*, *c* and *e*) and presence (spectra *b*, *d* and *f*) of PhCD. In Fig. 2 we summarize the changes in ^{1}H chemical shifts ($\Delta\delta_H$) of atenolol caused on interaction with PhCD in units of Hz at 600 MHz resonance frequency. As shown in this graph, all the protons of (*R*)-atenolol and protons a, b, e, e', f and g of (*S*)-atenolol shifted to a lower frequency as a result of interaction with PhCD; the extent of the low frequency shift was larger in (*R*)- than in (*S*)-atenolol, suggesting that the interaction of atenolol with PhCD was stronger in (*R*)- than in (*S*)-atenolol. This result agrees well with that found from elution order in an HPLC experiment using the PhCD column.[11] Interestingly, protons c, c', d and h of (*S*)-atenolol shifted to a higher frequency in contrast to the other protons. The low frequency shift of protons b, c, c' and d in (*R*)-atenolol and the high frequency shift of protons c, c' and d of (*S*)-atenolol appears to be responsible, respectively, for weakened and strengthened hydrogen bonding with the solvent molecules for the groups due to the OH, amine and CONH; the low frequency shift of the other protons can be considered as being due to the ring current effects arising from the phenyl groups of PhCD. It should be noted that in Fig. 1 the racemic atenolol also showed a low frequency shift on addition of PhCD (spectra e and f); furthermore, the extent of changes in the chemical shifts was larger than that observed for (*R*)-atenolol. This finding means that the low frequency shift in the (*R*)-enantiomer overwhelmed the high frequency shift in the (*S*)-enantiomer, indicating again that the interaction between atenolol and PhCD is stronger in the (*R*)- than in the (*S*)-enantiomers. Moreover, it should also be noted that the linewidths in spectrum b were slightly broader than those in spectrum d (compare the resonances due to proton c). These differences in linewidths suggest that the

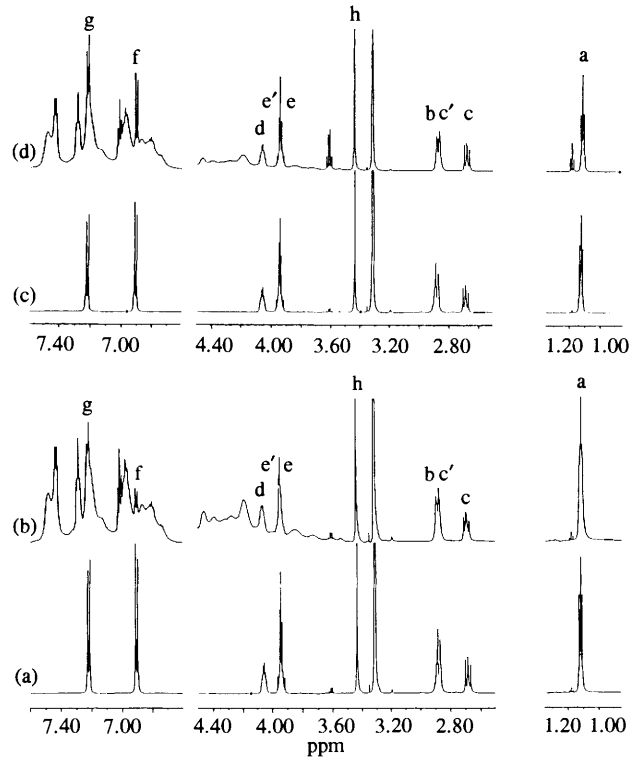

Fig. 3 ^{1}H NMR spectra of (*a*) 5 mmol dm^{-3} (*S*)-atenolol, (*b*) 5 mmol dm^{-3} (*S*)-atenolol and 5 mmol dm^{-3} PhCD, (*c*) 5 mmol dm^{-3} (*R*)-atenolol, (*d*) 5 mmol dm^{-3} (*R*)-atenolol and 5 mmol dm^{-3} PhCD solutions (283 K)

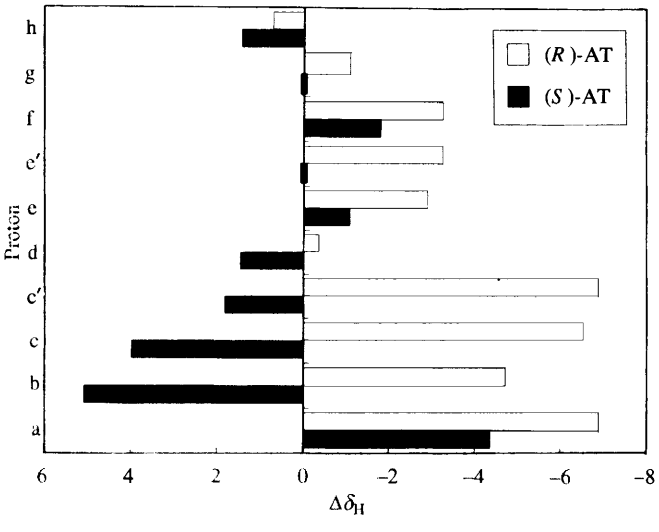

Fig. 4 Changes in chemical shifts of atenolol on interaction with PhCD (283 K)

mobility of (*S*)-atenolol is lower than that of the (*R*)-enantiomer in solutions containing PhCD; we noticed these differences in linewidths more clearly for the spectra at a low temperature (283 K). Although, at first sight, this result seems to be in conflict with the above mentioned understanding that the (*R*)-atenolol interacts with PhCD more strongly than the (*S*)-enantiomer, this paradox can be clearly settled by considering the following results of binding energy calculations. In contrast to these observations in atenolol, no appreciable changes in chemical shifts and linewidths were noted for protons due to PhCD; this finding seems to be due to many overlapping resonances of PhCD arising from protons of seven D-glucose and 21 phenylisocyanate units and the resulting fairly broad spectral lineshape.

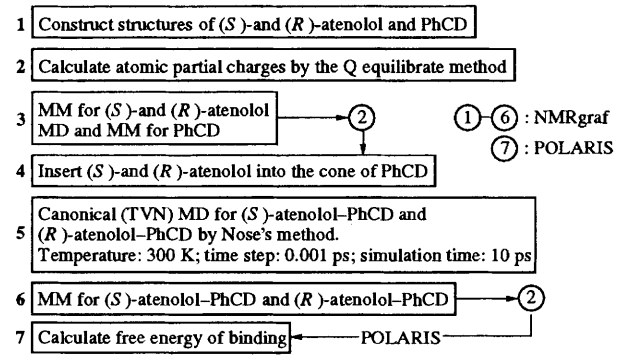

Fig. 5 Scheme of calculation of free energies of binding between atenolol and PhCD

^{1}H NMR spectra at 283 K

Fig. 3 shows ^{1}H NMR spectra of atenolol in the absence (spectra a and c) and in the presence (spectra b and d) of PhCD. Even at this low temperature the interaction between atenolol and PhCD was very weak. However, as in the case at room temperature, we could detect slight differences in chemical shifts of atenolol as summarized graphically in Fig. 4; the overall trend was the same as shown in Fig. 1, except that proton b of (*S*)-atenolol showed a high frequency shift. Once again, the racemic atenolol showed a larger, but entirely the same, trend of changes in chemical shifts as compared to the observations in (*R*)-atenolol–PhCD solution. Moreover, as mentioned above, we noticed clear differences in linewidths between (*S*)- and (*R*)-enantiomers. In Fig. 3, it is evident that all the proton resonances, including the aromatic ring of atenolol, were broader in the (*S*)- than in the (*R*)-enantiomer when the solutions contained PhCD. Accordingly, it can be concluded that although the binding affinity of (*S*)-atenolol is weaker than that of the (*R*)-enantiomer, the mobility of the (*S*)-enantiomer is lower than that of the (*R*)-enantiomer as a result of interaction with PhCD. In order to obtain information on the structures of the atenolol–PhCD complex which can satisfy all the findings in the ^{1}H NMR spectra, we performed molecular energy calculations.

Molecular mechanics (MM), molecular dynamics (MD) and free energy calculations †

The MM and MD calculations were performed by Molecular Simulations' NMRgraf (Ver. 3.1) software[12] running on a Silicon Graphics Iris INDIGO computer. The NMRgraf employs the DREIDING force field presented by Goddard III, *et al.*[13] Free energies were calculated by Molecular Simulations' POLARIS (Ver. 3.1) software. The theoretical background for the calculations of free energy is given by Warshel *et al.*[14–16] The scheme of calculations of free energies of binding between atenolol and PhCD is summarized in Fig. 5; steps 1–6 were performed by NMRgraf and step 7 was performed by POLARIS. The starting structures of (*S*)- and (*R*)-atenolol were constructed by using an organic molecule builder installed in the NMRgraf; a cationic form of atenolol was considered in the present work, because the HPLC experiments have been performed at acidic conditions.[11] The calculations of atomic partial charges were made by the charge (*Q*) equilibration method developed by Goddard III, *et al.*[17] Since PhCD is a sterically very crowded molecule, it was necessary to construct its structure stepwise. First, we constructed β-CD by using the

† Coordinates of atenolol and PhCD including atomic partial charges finally used for the molecular modellings in Tables 1–3 (Calc A) are available from the author on request.

Table 1 Calculated energies for four models (I–IV) of binding of (*S*)- and (*R*)-atenolol (AT) with PhCD[a]

	Model I		Model II		Model III		Model IV	
	(*R*)	(*S*)	(*R*)	(*S*)	(*R*)	(*S*)	(*R*)	(*S*)
Calc A								
AT[b]	0.974	0.540	0.842	0.952	0.597	0.551	0.512	0.367
PhCD[b]	0.026	0.459	0.158	0.048	0.403	0.448	0.487	0.633
Angles[c]	226.8	220.6	204.4	207.8	211.9	206.5	208.5	205.0
Torsions[c]	114.6	118.0	113.1	118.5	114.1	134.9	123.5	117.7
VdW[c]	377.6	380.2	368.2	386.5	359.4	365.2	371.2	377.9
Elec[c]	−718.0	−719.0	−692.3	−709.8	−700.0	−695.6	−704.1	−711.3
Hbond[c]	−107.6	−121.9	−117.7	−114.5	−92.6	−95.8	−104.4	−98.9
Total[c]	−33.4	−43.1	−52.7	−38.0	−35.0	−14.2	−35.6	−41.6
dG[d]	13.5	−9.7	10.8	32.5	19.1	21.4	4.8	8.4
Calc B								
Total[c]	−31.9	−35.3	−56.0	−39.0	−41.4	−19.4	−34.9	−44.6
dG[d]	16.3	−7.3	6.8	19.4	35.4	12.1	20.3	3.4

[a] Energies in kcal mol^{-1}. [b] Total charges for AT and PhCD molecules. In Calc B, the total charges are +1.0 for AT molecule and 0.0 for PhCD molecule. [c] Calculated by NMRgraf. Angles, bond angle bending energy; Torsions, dihedral angle torsion energy; Vdw, van der Waals interaction energy; Elec, electrostatic interaction energy; Hbond, hydrogen bond energy; Total, total energy in the MM calculation. [d] Calculated free energy of binding of (*S*)- and (*R*)-AT with PhCD.

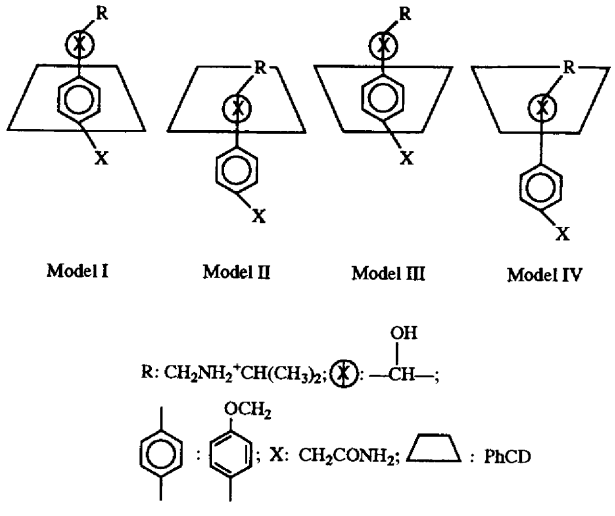

Fig. 6 Models of the binding between atenolol and PhCD

organic molecule builder and then performed MM calculations which include bond stretch, angle bend, torsion, electrostatic, van der Waals and hydrogen bond energies to obtain an energetically stable structure. Secondly, we replaced its secondary and primary hydroxy groups gradually by phenylcarbamate, repeating steps 2 and 3 in Fig. 5 several times. Lastly, for the complete PhCD molecule which includes 21 phenylcarbamate groups in all, MD and MM calculations were made for obtaining an energetically stable conformation; the calculations SCHEME 1 of NMRgraf which performs annealed MD and MM alternatively was employed here.

As an interaction model between atenolol and PhCD, we considered four kinds of binding modes as shown schematically in Fig. 6. In models I and II, we inserted the hydrophobic aromatic ring of atenolol into the cone of PhCD from its primary hydroxy group side to such an extent that the asymmetric carbon atom of the atenolol locates outside (model I) and inside (model II) the toroid of cyclodextrin. Conversely, in models III and IV, we inserted the atomic ring into the cone of PhCD from its secondary hydroxy group side; the extent of insertion corresponds to models I and II, respectively. To obtain energetically minimum conformations for these models of binding, a canonical MD of a constant temperature (300 K) and constant volume (TVN) was performed. This canonical dynamics method has an excellent characteristic in that it equilibrates a system much faster than the conventional microcanonical dynamics.[18] Accordingly, we employed a simulation time of 10 ps in the MD calculations; the time step was 0.001 ps and the Nose's method[19] was chosen. In fact, the calculated total energies almost converged within the 10 ps of simulation time. Thus, we extracted the energetically lowest structure at around the 10 ps from each trajectory file in the canonical MD calculations and then performed MM calculations for the extracted structure. For these energetically minimized structures of models I–IV, we re-calculated atomic partial charges, because the charges calculated from the Q-equilibration method depend on the molecular structure. In the re-calculation procedure of the atomic partial charges, we tried two kinds of calculation methods. One was to calculate the charges by involving both cationic atenolol and neutral PhCD molecules simultaneously (Calc A) and the other was to calculate the charges of the two molecules separately (Calc B). In Calc A, the +1 charge at the nitrogen of atenolol is distributed not only for the other atoms of an atenolol molecule but also for the atoms of a PhCD molecule; the net charges of atenolol and PhCD molecules for binding models I–IV are shown in Table 1. In Calc. B, on the other hand, the +1 charge is preserved within an atenolol molecule and thus the net charge on a PhCD molecule remains zero. By using newly calculated atomic partial charges on both Calc A and Calc B, we performed, again, MM calculations for (*R*)-atenolol–PhCD complexes of models I–IV and then subjected to the calculations of free energies of binding of atenolol to PhCD. The corresponding four kinds of structures of (*S*)-atenolol–PhCD complexes were each constructed by simply inverting the chirality of the (*R*)-atenolol–PhCD complexes at the step 4 and performed steps 5–7 in a similar manner as above. The computer graphics picture for the binding models I–IV are shown in Fig. 7. The calculated total energies and their relevant energies including bond angle bending (Angles), dihedral angle torsion (Torsions), van der Waals (VdW), electrostatic (Elec), and hydrogen bond (Hbond) are summarized in Table 1; in Calc B, items of each energy term are omitted, since no appreciable changes in relative magnitude among them were noted between Calc A and Calc B.

Free energies of binding (dG) were calculated by using a multiple run method which displaces the centre of a Langevin grid with a radius of 30 Å at random[15] and the results are

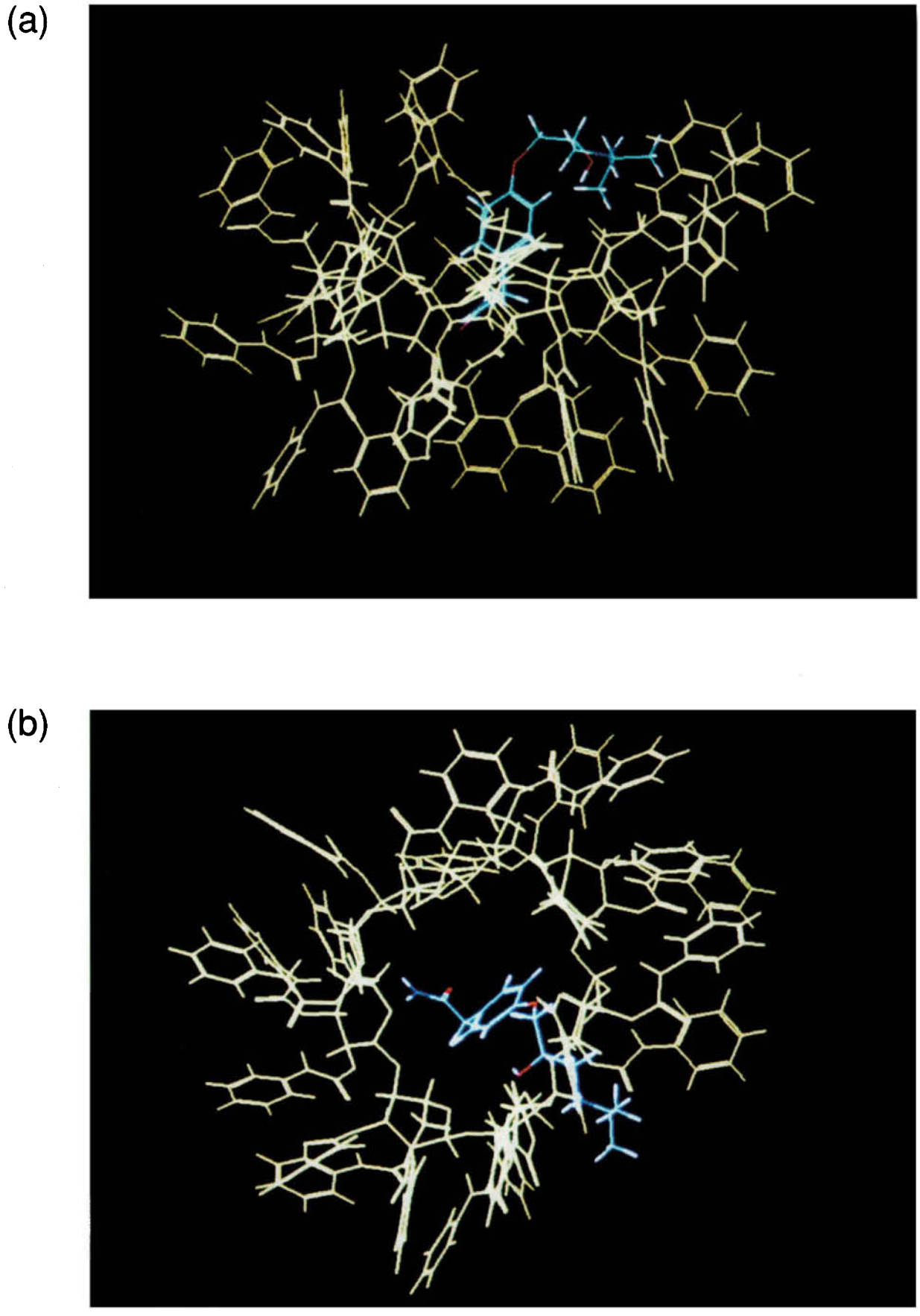

Fig. 7 Computer graphics view for the models I (a,b), II (c,d), III (e,f) and IV (g,h) of (*S*)-atenolol–PhCD complex. (a) and (c): viewed from the cone side of PhCD; primary hydroxy group side is shown upward. (e) and (g): viewed from the cone side of PhCD; primary hydroxy group side is shown downward. (b), (d), (f) and (h): overhead view from the primary hydroxy group side.

(c)

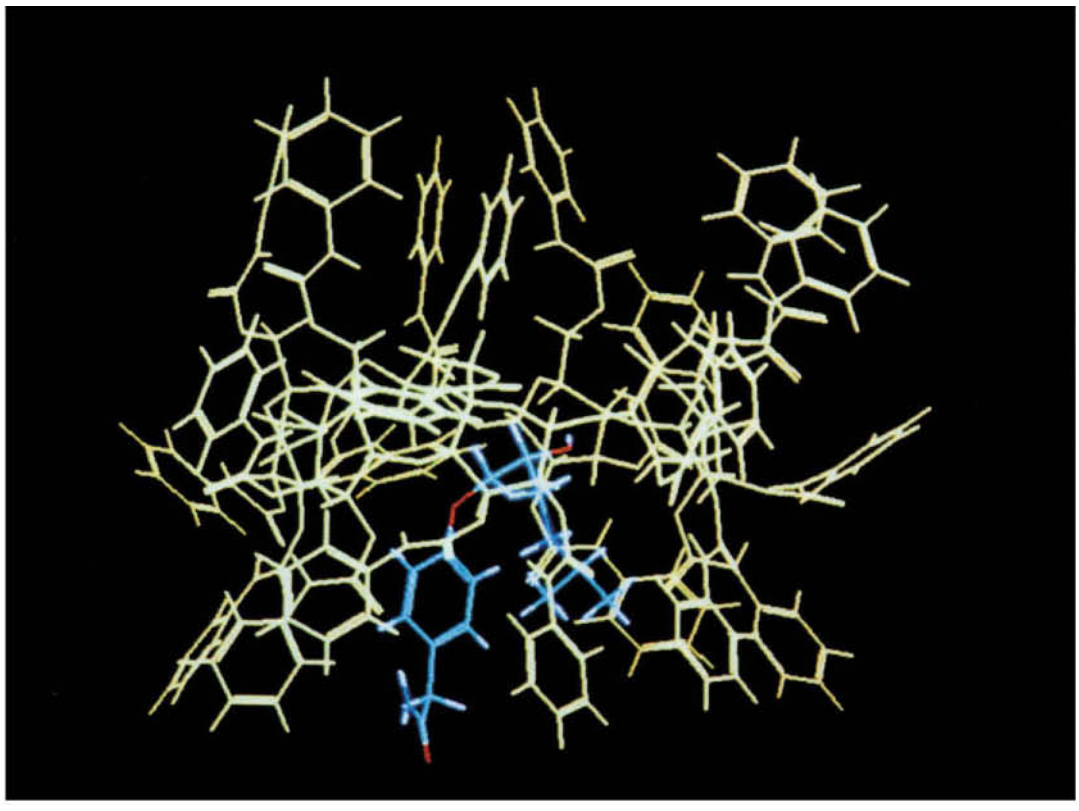

(d)

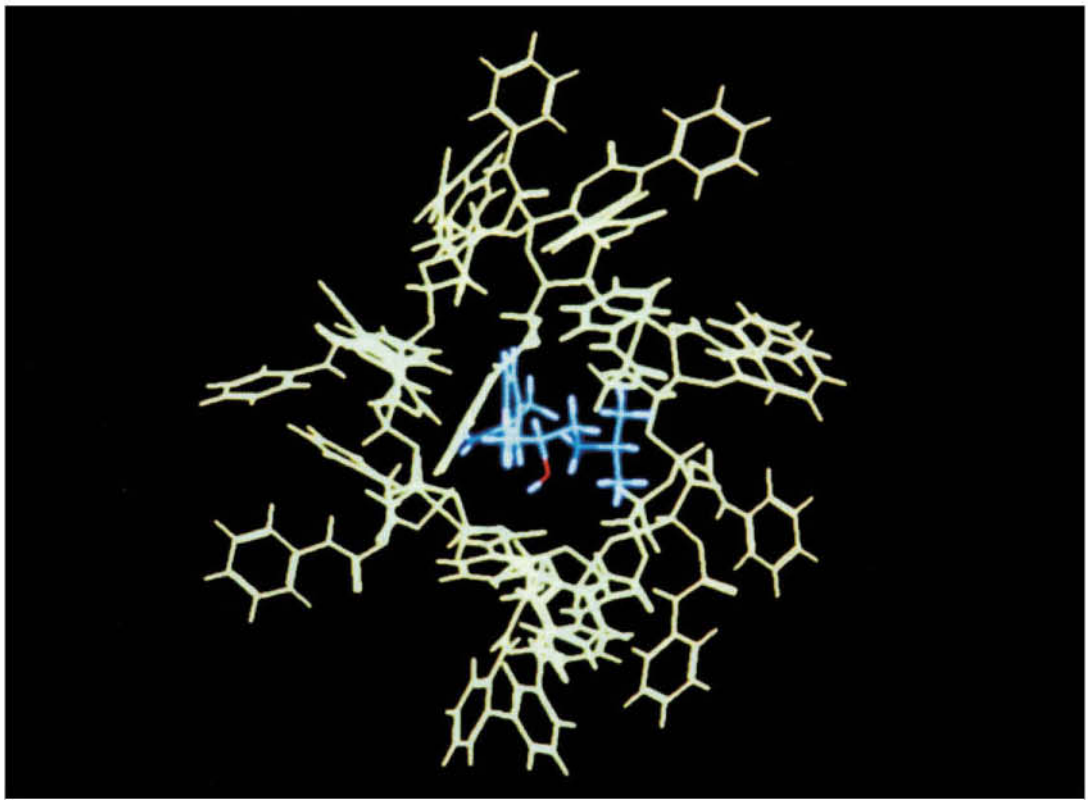

(e)

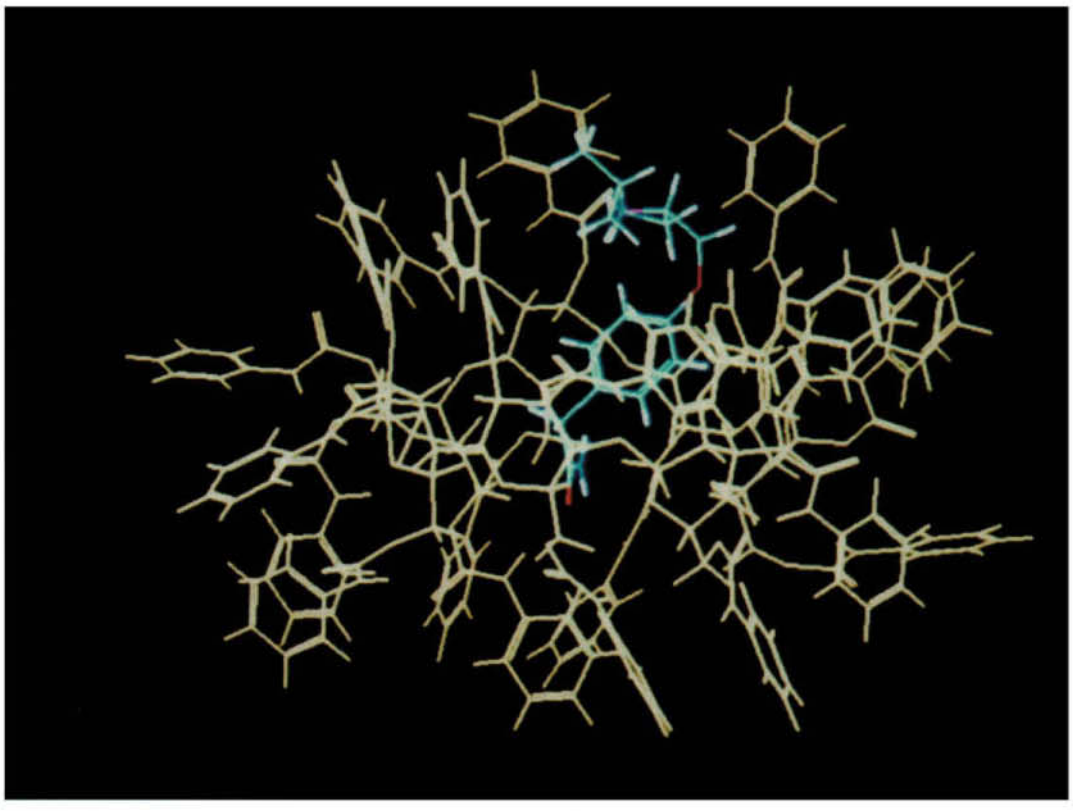

(f)

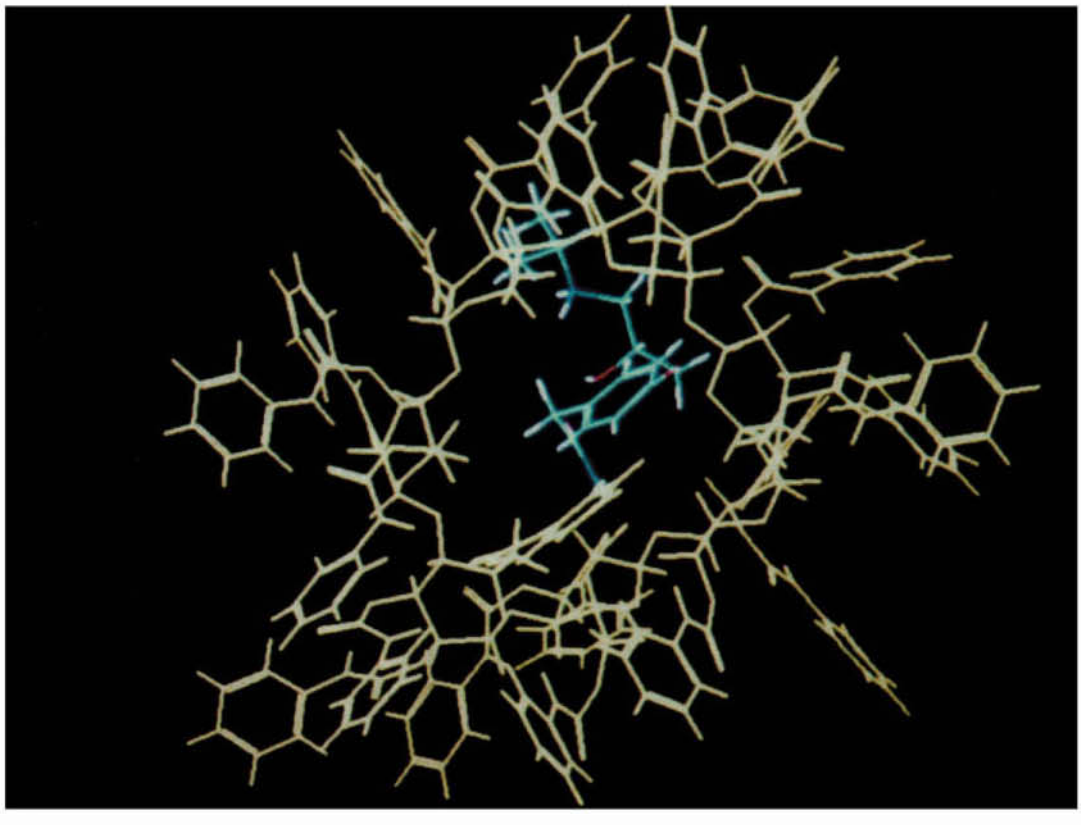

(g)

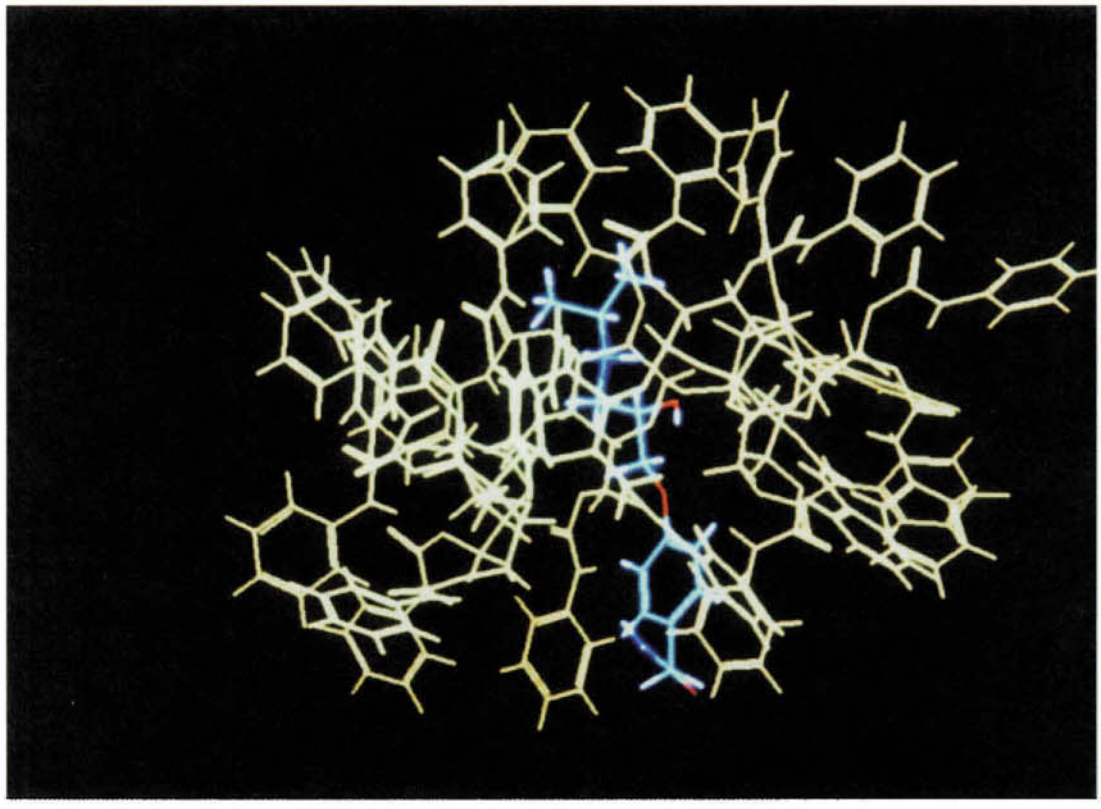

(h)

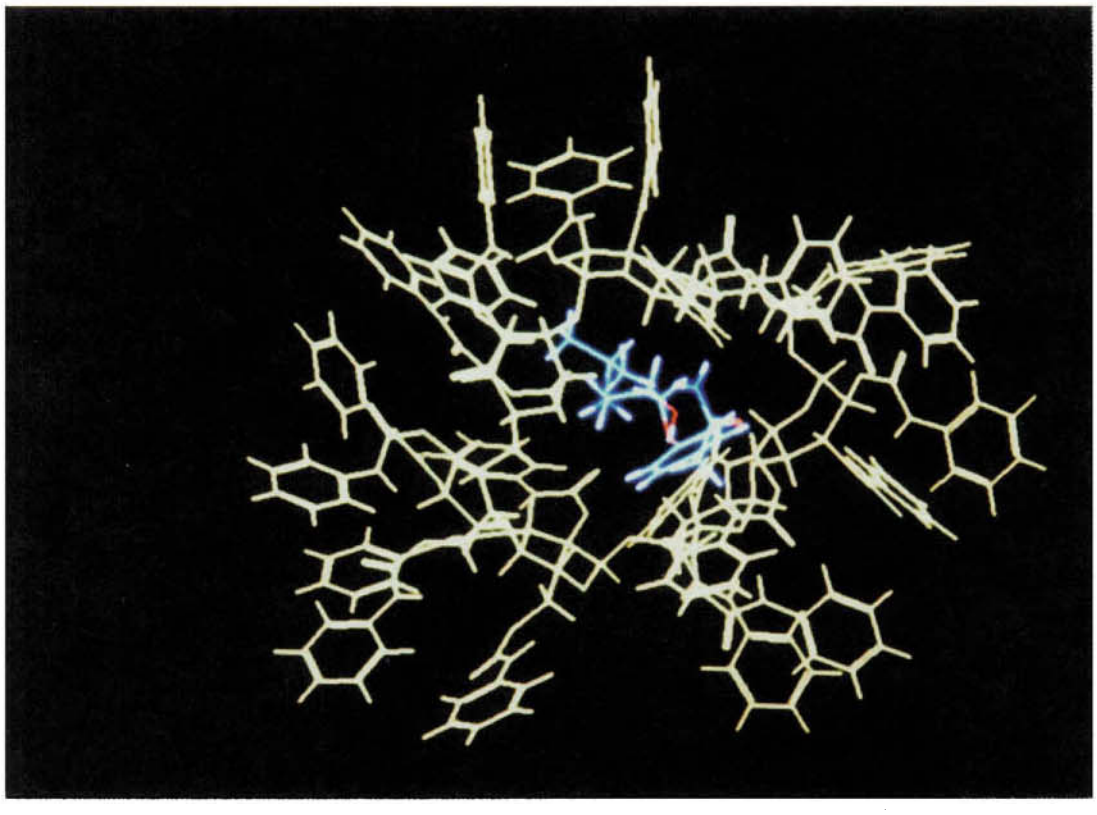

Table 2 Calculated energies for four solvated (methanol) models (I–IV) of binding of (*S*)- and (*R*)-atenolol (AT) with PhCD[a]

	Model I		Model II		Model III		Model IV	
	(*R*)	(*S*)	(*R*)	(*S*)	(*R*)	(*S*)	(*R*)	(*S*)
Calc A								
AT[b]	0.893	0.527	0.868	0.974	0.456	0.555	0.501	0.371
PhCD[b]	0.107	0.473	0.132	0.026	0.544	0.445	0.499	0.629
Solv[c]	264	274	276	255	264	277	275	267
Angles[d]	216.2	213.3	213.7	201.8	222.2	200.6	210.1	207.6
Torsions[d]	138.6	141.9	130.5	134.3	122.0	139.6	116.7	131.0
VdW[d]	382.3	384.9	375.1	391.7	365.1	379.8	381.0	375.7
Elec[d]	−734.6	−715.6	−697.3	−674.6	−691.2	−696.7	−693.5	−703.1
Hbond[d]	−109.6	−120.8	−123.8	−117.7	−100.0	−91.6	−101.2	−97.2
Total[d]	−32.6	−20.5	−30.9	5.2	−3.6	0.4	−17.7	−13.3
dG[e]	9.9	12.0	−1.0	11.1	22.0	33.9	8.7	11.6
Calc. B								
Total[d]	−8.1	9.8	−23.1	18.6	12.4	16.5	−2.5	−1.9
dG[e]	7.1	16.0	13.2	14.4	12.9	9.9	6.7	13.3

[a] Energies in kcal mol^{-1}. [b] Total charges for AT and PhCD molecules. In Calc B, the total charges are +1.0 for AT molecule and 0.0 for PhCD molecule. [c] Number of methanol molecules generated is shown here. [d] Calculated by NMRgraf. Angles, bond angle bending energy; Torsions, dihedral angle torsion energy; Vdw, van der Waals interaction energy; Elec, electrostatic interaction energy; Hbond, hydrogen bond energy; Total, total energy without solvent contribution in the MM calculation for a solvated model. [e] Calculated free energy of binding of (*S*)- and (*R*)-AT with PhCD.

Table 3 Calculated energies for four solvated (water) models (I–IV) of binding of (*S*)- and (*R*)-atenolol (AT) with PhCD[a]

	Model I		Model II		Model III		Model IV	
	(*R*)	(*S*)	(*R*)	(*S*)	(*R*)	(*S*)	(*R*)	(*S*)
Calc A								
AT[b]	0.978	0.576	0.855	0.923	0.607	0.523	0.467	0.384
PhCD[b]	0.021	0.424	0.145	0.077	0.393	0.476	0.532	0.616
Solv[c]	264	274	276	255	264	277	275	267
Angles[d]	230.6	221.3	202.6	213.2	204.6	194.1	219.2	208.5
Torsions[d]	136.2	132.7	123.4	135.8	142.6	166.9	130.9	137.3
VdW[d]	373.9	384.1	374.7	371.3	367.1	385.2	371.7	380.6
Elec[d]	−702.2	−693.0	−684.1	−675.3	−692.7	−691.8	−706.9	−709.1
Hbond[d]	−96.2	−119.6	−120.2	−117.3	−89.1	−101.1	−99.2	−93.3
Total[d]	14.1	−1.96	−29.9	2.28	5.10	24.7	−8.27	−3.16
dG[e]	4.48	6.41	−5.97	5.34	27.0	7.38	6.51	22.7
Calc B								
Total[d]	38.8	25.5	−19.6	25.3	14.5	42.6	15.9	15.2
dG[e]	14.1	8.05	−4.57	6.42	18.6	7.67	4.84	3.66

[a] Energies in kcal mol^{-1}. [b] Total charges for AT and PhCD molecules. In Calc B, the total charges are +1.0 for AT molecule and 0.0 for PhCD molecule. [c] Number of water molecules generated is shown here. [d] Calculated by NMRgraf. Angles, bond angle bending energy; Torsions, dihedral angle torsion energy; Vdw, van der Waals interaction energy; Elec, electrostatic interaction energy; Hbond, hydrogen bond energy; Total, total energy without solvent contribution in the MM calculation for a solvated model. [e] Calculated free energy of binding of (*S*)- and (*R*)-AT with PhCD.

summarized in Table 1. We used five optimal centres out of 15 trials of the Langevin grid centre and then subjected to computation Boltzman averages of the POLARIS energy terms; the total number of self-consistent iterations to be carried out in the free energy calculations was set to 15, however the calculations usually converged within ten iterations.[15]

The MM and MD calculations for a solvated model have been made starting from each of the finally calculated structures in the unsolvated models of I–IV. The solvents chosen were methanol and water to match the present NMR and the previous HPLC experimental conditions,[11] respectively. The type of grid which holds the solvent molecule was diamond and the inner and the outer cutoff distances for the solvent to be generated were 2.8 and 5.6 Å, respectively. The number of solvent molecules generated in each model is shown in Tables 2 and 3. The calculations of atomic partial charges for the solvent molecules were made by the Gasteiger method.[20] For a model thus prepared, we initially performed MM calculations and then subjected to MD, MM, and finally free energies of binding calculations as in the steps 5, 6 and 7 for the unsolvated models (Fig. 5). Calculated energies are summarized in Tables 2 and 3. Since the number of solvents generated in each model differed from one another, no contributions from the solvent molecules are included for the bond angle bending, dihedral angle torsion, van der Waals, electrostatic, hydrogen bond, and total energy values in Tables 2 and 3.

It should be mentioned that the total energies given by NMRgraf may be compared among four models employed presently. On the other hand, the dG values by POLARIS can be used to discuss which enantiomer is more favourable within the binding model assumed presently, because no consideration due to the entropy change of a system owing to the binding of atenolol with PhCD was paid in the present dG calculations; we used the dG values in the following discussion by assuming that the changes in entropy term are the same between the two enantiomers within a given binding model. This assumption

may be rationalized, because we want to compare the dG values between closely related substrates, that is, those having enantiomeric relationship with each other.[21] Also, any deficiencies in the force field will be the same for both enantiomers and thus nearly the same for both PhCD complexes.[22]

Discussion

Cyclodextrins and derivatized cyclodextrins are known to be useful chiral NMR shift reagents and thus have been used for studying enantiorecognition.[22–26] Equivalent protons of both enantiomers of a chiral molecule give resonances which differ in chemical shift after interaction with the cyclodextrins or with the derivatized cyclodextrins. The resonances of the racemate appear in duplicate form. Here, in all the observations so far reported, the equivalent protons shifted to the same direction as compared to their original chemical shift value. This implies that the interaction between the chiral molecule and cyclodextrin is occurring at the same region but to a differing degree. In contrast, our present data involve three important findings: (1) some equivalent protons of enantiomers, especially those at around the polar groups of atenolol shifted in an opposite direction (Figs. 2 and 4); (2) the resonances of the racemate did not appear in duplicate form (Fig. 1); and (3) the linewidths for protons of (*S*)-enantiomer became broader than those of (*R*)-antipode, although the magnitude of changes in chemical shift informed us that the (*R*)-enantiomer interacted with PhCD more strongly than the (*S*)-antipode. The finding (2) simply tells us that the binding of atenolol to PhCD was very weak and thus the exchange was very fast in the present experimental condition. However, the findings (1) and (3) cannot be simply interpreted by imaging the binding of atenolol with PhCD at the same region. We should consider different structures of the complex with PhCD for the two enantiomers.

In order to gain insight into the difference in the structure or the difference in the binding mode between enantiomers, we have performed molecular energy calculations by assuming four plausible structures of the complex between atenolol and PhCD. Inspection of Table 1 indicates that in both Calc A and Calc B, the total energy of atenolol–PdCD complexes was the lowest for (*R*)-atenolol in the binding model II, suggesting that this binding model is energetically the most stable one for the (*R*)-enantiomer; while the total energy was the highest in model I, suggesting that the binding model I is the most unstable one for the (*R*)-enantiomer. In contrast, the total energy for the (*S*)-enantiomer–PhCD complex was the lowest in model I followed by model IV in Calc A. In Calc B, the (*S*)-enantiomer showed the lowest value in model IV. In both Calc A and Calc B the model III showed the highest total energy for the (*S*)-enantiomer–PhCD complex, suggesting that this model is energetically the most unstable one for the (*S*)-enantiomer. Thus, the (*S*)-enantiomer can be considered to prefer the binding models I and/or IV. The free energy of binding (dG) or (*R*)-atenolol in Calc A was lower than that of the (*S*)-enantiomer for binding models II, III and IV, although those energies were positive values. In model I, however, the reverse trend was noted and the dG value even became a negative value in the (*S*)-enantiomer, indicating that this model is the most unlikely one for the (*R*)-enantiomer, but the most likely one for the (*S*)-enantiomer. In Calc B, only the binding model II showed a lower dG value for the (*R*)-enantiomer than that for the (*S*)-enantiomer. Combining the results from consideration of total energies of the complexes with those from free energies of binding, we may conclude that (*R*)-atenolol binds with PhCD in such a manner as shown in model II; while the corresponding (*S*)-enantiomer binds with PhCD in such a manner as shown in model I. The difference in the binding mode between the enantiomers can be considered to be responsible for the chiral separation in an HPLC experiment with the PhCD column and also can explain all the findings from the ^{1}H NMR spectra. In the binding model II, the asymmetric carbon atom of atenolol locates inside the toroid of cyclodextrin. In this situation, the hydrogen bonding of the groups due to the OH and amine of atenolol with the solvent molecules would be fairly interrupted; this reduced hydrogen bond energy can be ascribed to the low frequency shift of protons b, c, c′ and d of (*R*)-atenolol as a result of interactions with PhCD. In the (*S*)-enantiomer, on the other hand, the binding model I is the most likely structure. In this situation the groups due to the OH and amine can form hydrogen bonding with the O–C=O–NH group of PhCD. In fact, the calculation indicated the largest negative hydrogen bond energy value for the (*S*)-atenolol–PhCD system in the binding model I. The high frequency shift of protons c, c′ and d of (*S*)-atenolol suggests that those hydrogen bonds with PhCD are stronger than with the solvent molecules. The binding model IV for (*S*)-atenolol suggested as a plausible candidate from the total energy value in Calc B cannot explain the high frequency shifts of protons b, c, c′ and d; thus this model should be denied. The mobility of atenolol molecules can be considered to be more restricted in the binding model I than in model II, because (1) these hydrogen bondings with PhCD will fix the atenolol molecule and (2) the aromatic ring is trapped in the toroid of cyclodextrin receiving repulsive forces from the surrounding glucose molecules; on the other hand, no such holding force is expected for an atenolol molecule in the binding model II. This difference in the binding mode between (*S*)- and (*R*)-enantiomers can clearly explain why the (*S*)-enantiomer–PhCD complex gave broader linewidths in its ^{1}H NMR spectrum than the (*R*) counterpart. Interestingly, we noticed in Fig. 7(*c*) that the conformation of the (*R*)-atenolol molecule is kinked around the asymmetric carbon moiety, directing its quaternary ammonium nitrogen moiety toward the secondary hydroxy group side, although the initial structure has been set such a manner as shown for model II in Fig. 6. Since the secondary hydroxy group side is wider in space than the primary hydroxy group side, the (*R*)-atenolol molecule in the binding model II can thus be considered to be relatively loosely packed into a PhCD molecule.

The total energies reported in Table 1 are all for models in a vacuum. Thus, in order to examine possible solvent effects on the energy values, we tried MM and MD calculations by solvating the finally determined structures in the unsolvated models (Tables 2 and 3). In Table 2, where the solvent is methanol, the most noteworthy differences in the energy values between those of the solvated and unsolvated models were that the total and dG values in all the models, except the dG value for model III in Calc B, resulted in lower values for (*R*)-enantiomer than for (*S*)-antipode, agreeing well with the result that (*R*)-atenolol interacts with PhCD more strongly than the (*S*)-antipode. The total and dG values, again favoured model II as a preferable binding mode of (*R*)-atenolol. However, in contrast to the finding in the unsolvated model, the solvated model also favoured model I for the (*R*)-enantiomer. Inspection of items in the total energy informs us that this is due to the lower electrostatic interaction energy in the (*R*)-enantiomer than in the (*S*)-antipode. Indeed, the Elec value became the lowest among all the models tested. The trends described for the unsolvated models that model I in Calc A and model IV in Calc B give the lowest total energy values for the (*S*)-enantiomer and also that the model I gives the lowest hydrogen bond energy for (*S*)-enantiomer, did not change on solvation by methanol. Thus, these findings support the discussion given above for the NMR data. Interestingly, solvation by water molecules showed much more clearly, that the (*R*)-enantiomer prefers to bind with PhCD in the binding model II. This result was reflected in both

total and dG values and also in both Calc A and Calc B (Table 3). The origin of the lowest total energy value for the (*R*)-enantiomer in model II can be ascribed to the relatively lower energy values in angles, torsions and Hbond terms as compared to the other binding models. Furthermore, we found that the relatively lower energy values in angles and torsions originate from PhCD, and not from atenolol (the data not shown in Table 3). These findings also apply to the results for the unsolvated model shown in Table 1. Table 3 also predicts the binding model I and/or IV as a plausible binding mode for the (*S*)-antipode. The total energy values in Calc A and Calc B showed again, that the binding model III is the most unlikely one for the (*S*)-antipode, as in Table 1. Summarizing the discussion for the solvated models, the calculated energies always support the binding model II for the (*R*)-atenolol, agreeing well with the result for the unsolvated models. On the other hand, the solvated models did not always offer a comfortable home to the (*S*)-antipode, although the binding models I and/or IV gave the possibility of binding for the (*S*)-antipode.

Our present calculations are not inclusive in that we assumed only four binding models I–IV. Lipkowitz *et al.* have reported a more inclusive method for delineating interaction between chiral molecules with chiral stationary phases or with cyclodextrins.[22,27] Moreover, the DREIDING force field employed presently is so determined as to predict equilibrium geometries of organic, biological and main-group inorganic compounds.[13] Thus, this force field may not be the best for treating molecules docking with each other. However, as described above, the binding models I and II in our calculations could clearly explain all the presently obtained findings in the NMR data. Thus, we may be allowed to conclude that the difference in the structures of a complex taking a minimum energy state in each enantiomer can be the origin of the enantiorecognition of PhCD–bonded silica column for atenolol and that the difference in the structures of complex was caused by phenylcarbamoylating the original cyclodextrin.

References

1 E. J. Ariens, *Clin. Pharmacol. Ther.*, 1987, **42**, 361.
2 E. J. Ariens, E. W. Wuis and E. J. Veringa, *Biochem. Pharmacol.*, 1988, **37**, 9.
3 M. J. Wilson, K. D. Ballard and T. Walle, *J. Chromatogr.*, 1988, **421**, 222.
4 S. K. Chin, A. C. Hui and K. M. Giacomini, *J. Chromatogr.*, 1989, **489**, 438.
5 R. Mehvar, *J. Pharm. Sci.*, 1989, **78**, 1035.
6 M. T. Rosseel, A. M. Vermeulen and F. M. Belpaire, *J. Chromatogr.*, 1991, **568**, 239.
7 R. B. Miller and Y. Guertin, *J. Liq. Chromatogr.*, 1992, **15**, 1289.
8 M. Enquist and J. Hermansson, *Chirality*, 1989, **1**, 209.
9 G. Egginger, W. Lindner, S. Kahr and K. Stoschitzky, *Chirality*, 1993, **5**, 505.
10 D. W. Armstrong, S. Chen, C. Chang and S. Chang, *J. Liq. Chromatogr.*, 1992, **15**, 545.
11 J. He, A. Shibukawa, T. Nakagawa, H. Wada, H. Fujima, E. Imai and Y. Go-oh, *Chem. Pharm. Bull.*, 1993, **41**, 544.
12 Molecular Simulations, Inc., 796 North Pastoria Avenue, Sunnyvale, CA 94086, USA.
13 S. L. Mayo, B. D. Olafson and W. A. Goddard III, *J. Phys. Chem.*, 1990, **94**, 8897.
14 A. Warshel and J. Aqvist, *Annu. Rev. Biophys. Chem.*, 1991, **20**, 267.
15 S. T. Russell and A. Warshel, *J. Mol. Biol.*, 1985, **185**, 389.
16 F. S. Lee, Z-T. Chu, M. B. Bolger and A. Warshel, *Protein Engineering*, 1992, **5**, 215.
17 A. K. Rappe and W. A. Goddard III, *J. Phys. Chem.*, 1991, **95**, 3358.
18 T. Cagin, W. A. Goddard III and M. L. Ary, *Comput. Polymer Sci.*, 1991, **1**, 241.
19 S. Nose, *J. Chem. Phys.*, 1984, **81**, 511.
20 J. Gasteiger and M. Marsili, *Tetrahedron*, 1980, **36**, 3219.
21 W. Clark Still, in *Computer Aided Innovation of New Materials II*, eds. M. Doyama, J. Kihara, M. Tanaka and R. Yamamoto, Elsevier, Amsterdam, 1993, pt. 1, p. 813–816.
22 K. B. Lipkowitz, S. Raghothama and J.-an Yang, *J. Am. Chem. Soc.*, 1992, **114**, 1554.
23 D. D. MacNicol and D. S. Rycroft, *Tetrahedron Lett.*, 1977, 2173.
24 D. Greatbanks and R. Pickford, *Magn. Reson. Chem.*, 1987, **25**, 208.
25 A. F. Casy and A. D. Mercer, *Magn. Reson. Chem.*, 1988, **26**, 765.
26 A. Taylor, D. A. R. Williams and I. D. Wilson, *J. Pharm. Biomed. Anal.*, 1991, **9**, 493.
27 K. B. Lipkowitz, D. A. Demeter, R. Zegarra, R. Larter and T. Darden, *J. Am. Chem. Soc.*, 1988, **110**, 3446.

Paper 5/01369K
Received 6*th March* 1995
Accepted 19*th May* 1995